Revista Mexicana de Astronomía y Astrofísica, **43**, 95–100 (2007)

MORPHOLOGY AND KINEMATICS OF GRAVITATIONAL COLD COLLAPSE AROUND A CENTRAL SUPERMASSIVE BLACK HOLE

Fidel Cruz, Héctor Velázquez, and Héctor Aceves

Instituto de Astronomía
Universidad Nacional Autónoma de México, Ensenada, B. C., Mexico

Received 2006 March 16; accepted 2006 October 13

RESUMEN

Estudiamos las propiedades morfológicas y cinemáticas de sistemas triaxiales formados por colapso gravitacional usando simulaciones de N-cuerpos. Se consideran dos modelos; en uno de ellos el agujero negro supermasivo (SBH) ya existe antes del colapso gravitacional; en el otro caso el SBH crece de manera adiabática después de que el sistema se ha colapsado y se encuentra en equilibrio virial. El análisis de las isofotas de densidad a lo largo de los ejes principales muestra que la presencia del SBH tiende a hacer las isofotas más rectangulares que cuando no hay SBH. Los resultados de la cinemática utilizando la expansión de Gauss-Hermite muestran que la dispersión de velocidades central aumenta en presencia del SBH, y permanece constante para modelos sin SBH. El parámetro h_4 es positivo dentro del radio de influencia del SBH, y cambia de signo fuera de esta región. Para el modelo sin SBH $h_4 > 0$ a todos los radios. De estos resultados concluimos que no es posible distinguir entre ambos modelos.

ABSTRACT

Using N-body simulations we study the morphological and kinematical properties of triaxial systems formed through cold gravitational collapses. Two models are considered; in one case, the supermassive black hole SBH already exists before the gravitational collapse, and in the other the SBH grows adiabatically after the collapsed system has reached virial equilibrium. Isophotal analysis along the principal projected axes shows that the SBH tends to make the isophotes more boxy than in the case without a central SBH. Also, the kinematics obtained from a Gauss-Hermite expansion shows that the central velocity dispersion increases in presence of the SBH while it remains almost constant for models without a SBH. Furthermore, the h_4 parameter is positive inside the radius of influence of the central black hole while it is negative beyond of this region. For models without a SBH $h_4 > 0$ at all radii. Finally, from these results we conclude that is not possible to distinguish between both models.

Key Words: **GALAXIES: ELLIPTICAL — GALAXIES: FORMATION — GALAXIES: NUCLEI — METHODS: NUMERICAL**

1. INTRODUCTION

Observations indicate that elliptical galaxies can broadly be divided into two distinct groups according to their morphological and kinematical properties. On one hand, faint ellipticals are characterized by a power-law inner density profile and disky-like isophotes. They appear isotropic and mostly supported by rotation. On the other hand, bright ellipticals exhibit an inner central core, boxy isophotal shapes, and are mainly supported by anisotropy. Furthermore, they show a slow rotation along the major axis in comparison to the minor axis (Bender 1988; Jaffe et al. 1994; Faber et al. 1997; Lauer et al. 2005).

Observations of ellipticals with higher central resolutions indicate that their central part is dominated by a supermassive black hole (Kormendy & Richstone 1995; Kormendy & Gebhardt 2001). It is accepted that central black holes should have a substantial influence on the dynamics and evolution of the surrounding stars inside of a radius of influence $r_{bh} = GM_{bh}/\sigma^2$, where M_{bh} is the black hole mass and σ the central velocity dispersion of the host galaxy. Current dynamical estimates of black hole masses (Magorrian et al. 1998; McLure & Dunlop 2002; Marconi & Hunt 2003) and the central velocity dispersions (Ferrarese & Merritt 2000; Gebhardt et al. 2000) suggest an intimate connection between the origin of these massive objects and the formation of the galaxy itself.

Faber et al. (1997) drew a basic picture to try to understand this dichotomy in shape and velocity. They proposed that central power-law galaxies were formed through a dissipative process accompanied by a period of star formation, while those galaxies with a core were produced by mergers of power-law galaxies harboring a central black hole. In this last case, the black hole forms a hard binary at the final stages of the merger, ejecting stars from the central region and leading to the formation of a core. Thus, central power-law profiles were sites dominated by dissipation, and cores were dominated by mixing and scattering (Lauer et al. 2005).

Mergers of disk galaxies without a central black hole have been extensively studied (Naab, Burket, & Hernquist 1999; Cretton et al. 2001; Naab & Burkert 2003). It is found that about one-half of the projected remnants of equal-mass mergers is boxy ($a_4 < 0$) and the other half shows disky isophotes ($a_4 > 0$). Also, they are slow rotators. In the case of unequal-mass mergers, a disky isophote signature ($a_4 > 0$) and a fast rotation can be observed (Naab & Burkert 2003). Recently, Khochfar & Burkert (2005) using semi-analytical models concluded that equal-mass mergers lead to boxy ellipticals while unequal-mass mergers produce disky galaxies. They suggested a division for boxy ellipticals in such a way that equal-mass mergers of ellipticals yield power-law density profiles and disk galaxy mergers tend to produce core-like profiles. In contrast with this proposal, Milosavljevic & Merritt (2001) found that the remnants of equal-mass mergers of ellipticals harboring a central black hole exhibit a central core.

An alternative scenario to form triaxial systems with a de Vaucouleurs $R^{1/4}$ profile is through gravitational cold collapse (*e.g.* van Albada 1982, Aguilar & Merritt 1990, Udry 1993). The aim of this paper is to study the morphology and kinematics of triaxial systems in the context of isolated gravitational cold collapses using numerical simulations. Two possible mechanisms will be addressed: (a) the collapse occurs around a primordial supermassive central black hole, and (b) the black hole grows adiabatically once the inner region of the system has relaxed. The rest of the paper has been organized as follows: Section 2 provides a description of the initial conditions and the integration code used to carry out our numerical simulations. The morphological analysis, the resulting Fourier coefficient a_4 and the projected ellipticity e are given in Section 3. Section 4 contains the kinematical analysis. Here, the velocity distribution, the velocity dispersion and the parameter h_4 along the principal axes of the resulting triaxial system are derived for all our simulations. Finally, our main conclusions are given in Section 5.

TABLE 1

SIMULATION PARAMETERS

Simulation	M_{bh}/M_{gal} ($\times 10^{-2}$)	t_{growth}	N ($\times 10^3$)
NBH00	0.0	···	32
NBH01	0.0	···	64
PBH00	1.0	···	32
PBH01	1.0	···	64
ABH00	1.12	15	32
ABH01	1.12	15	64

2. METHODS

In this section we briefly describe the methods to set up the initial conditions, as well as the code used to follow the evolution of the collapses with emphasis on the central region, where the supermassive black hole is supposed to reside. Two particular mechanisms are explored, one where the central black hole has a primordial origin, and the other where this central object grows adiabatically once the inner zones of the system have collapsed and relaxed.

2.1. *NHB: Galactic Cold Collapse without a BH*

We set the positions of a gravitational cold collapse from an initial power-law density profile $\rho \propto r^{-1}$ and the velocities are randomly drawn from an isotropic Maxwellian distribution. The initial virial ratio for these simulations is given by $\eta = 2T/|W| = 0.05$ where T and W are the total kinetic and potential energy, respectively. In all cases, the simulations consist of 32000 and 64000 equal-mass particles (see fourth column of Table 1). A system of units has been chosen where $M_T = 1$, $G = 1$, and the total energy is $E = -1/4$. With this system of units the free-fall timescale, t_{ff}, is about 5 time units.

To study the effects and importance of a central black hole on the morphology and kinematics of a gravitational collapse we have followed its evolution in absence of the central black hole for about $15\,t_{ff}$.

2.2. *PBH: A Primordial Black Hole*

In this model, the supermassive black hole exists before the collapse occurs. No attempt is made to explain the formation of a such central object; this is beyond the scope of the present paper. The mass of this massive object is $M_{bh} = 0.01 M_t$, where M_t is the total mass of the collapsing sphere (see second column of Table 1). The evolution of the model is followed for about $5\,t_{ff}$. After this time, the central region has completely relaxed.

2.3. *ABH: Adiabatic Growth of a Black Hole*

The other model corresponds to the case where the central black hole grows adiabatically once the central parts of the gravitational cold collapse, without a black hole, have relaxed for about $5t_{ff}$ (see models NBH00 and NBH01 in Table 1). At this time, they exhibit an inner density core with a power-law index of about 0.2 (Cruz & Velázquez 2005). Using the prescription from Merritt & Quinlan (1998), the adopted growth rule for the central mass is:

$$\begin{aligned} M(t) &= M_{bh}\tau^2(3-2\tau), \tau \leq 1, \\ &= M_{bh}, \qquad\qquad\quad \tau > 1, \end{aligned} \tag{1}$$

where $\tau = t/t_{grow}$ and t_{grow} is the growth time. For this set of simulations we adopted a mass of $M_{bh} = 0.01$ as an initial "seed" and $t_{grow} = 15$. Once t_{grow} is reached, the system is allowed to relax for another $7t_{ff}$ (models ABH00 and ABH01 in Table 1).

The observed frequency distribution of black hole to spheroid/bulge component mass ratios $N[\log(M_{bh}/M_b)]$ is well described by a Gaussian with $M_{bh}/M_b \approx 0.00125$ with a standard deviation of 0.45 (Merritt & Ferrarese 2001, McLure & Dunlop 2002). Direct numerical simulations present a challenge due to the CPU time that scales as N^2 and imposes a limit to N. If we introduce a realistic black hole mass with 32k and 64k particles in this simulation, the black hole to particle mass ratio is $M_{bh}/m_p = 32$ or 64, that is, very unrealistic. The observation show that $\log(M_{bh}/m_p)$ is $\sim$ 6–9. For this reason we decided to use $M_{bh} = 0.01 M_t$ so as to increase the black hole to particle mass ratio by an order of magnitude.

2.4. *The N-body code*

For the evolution of these simulations we use a direct-summation Systolic code. This code combines a fourth-order Hermite integrator with an individual time-step scheme for each particle; time steps are controlled by an accuracy parameter (Dorban, Hemsendorf & Merritt 2001). These combined properties allow us to follow with enough accuracy a large spatial and temporal dynamic range. This is even more important in the inner regions, where the orbits of the particles inside the black hole's radius of influence need to be integrated with high accuracy. The collisionless nature of this system is guaranteed using a reasonably large number of particles to avoid numerical artifacts during the simulation time. For our simulations the time evolution of the Lagrangian radii remains in steady state for several crossing times after the cold collapse with 32k and 64k particles (Cruz & Velázquez 2005).

This code has been optimized for parallel computers with the Message Passing Interface (MPI) libraries. In all cases, the energy conservation was better than 0.001%. These numerical simulations were performed on a cluster consisting of 32 Pentium III (450 MHz) processors (Velázquez & Aguilar 2003). A single simulation with 64000 particles takes about 2 months of CPU time on this cluster.

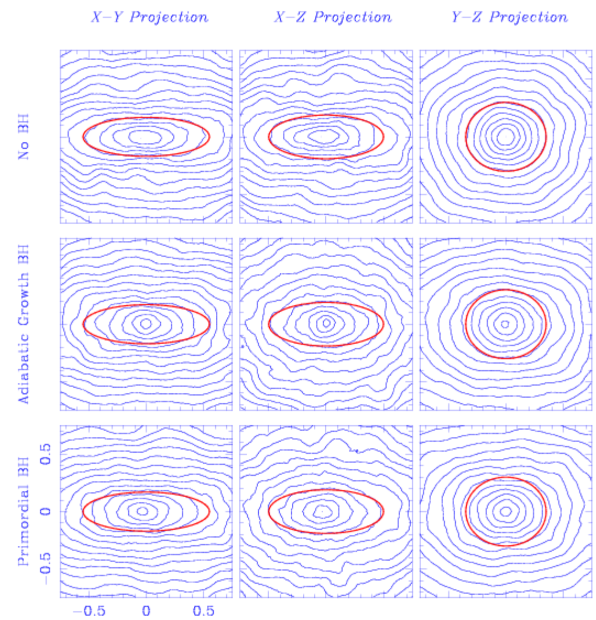

Fig. 1. Projected contours of the mass density along the principal axes for our models NBH01, ABH01 and PBH01 (from top to bottom).

3. MORPHOLOGY

Figure 1 shows the projected contours of the mass density along the principal axes at the end of our higher resolution simulations listed in Table 1. Top panels correspond to our model ABH01, middle ones to model PBH01 and bottom panels to the adiabatically growing case NBH01. In order to improve the Poisson noise these contours were computed by superposing eight snapshots with a time separation between them of 0.1 time units. No significant change of density profiles was observed in this period. Also, an adaptive kernel window was used in order to smooth these contours (Green & Silverman 1994). To illustrate any deviations from a perfect ellipse, a best fitted ellipse (thick line) to one of the contours for each projection of our simulation NBH01 has been plotted in all frames as a reference.

It can be seen that the central regions of models PBH01 and ABH01 are nearly spherical in all projections. Notice that despite the fact that the black hole is confined to the center of the triaxial system, its effect can be traced beyond small radii, where larger deviations from an ellipse can be observed in comparison with model NBH01.

To quantify these deviations, i.e., the boxiness ($a_4 < 0$) or diskness ($a_4 > 0$) of the isophotes, we create a FITS image summing five projected density contour plot images separated in time by 0.1 model units. This done, the parameter a_4 is computed by using the isophote package of the Space Telescope Science Data Analysis Software (STSDAS) included in IRAF. These routines also allow us to determine the ellipticity of the isophote along the major semi-axis of the fitted ellipse, defined as $\epsilon = 1 - b/a$, where a and b are the major and minor semiaxes of the fitted ellipse.

The results of this fitting process are given in Figures 2 and 3. Top, middle and bottom panels of Figure 2 indicate the degree of boxiness or diskness of models NBH01, ABH01 and PBH01, respectively. By comparing Figure 1 and Figure 2, it can be seen that boxy contours have negative values of a_4 and disky contours have positive values, as expected.

Figure 3 shows the ellipticity of the final systems as a function of the distance along the semi-major axis for models PBH01 (top panel, line with error bars) and ABH01 (bottom panel, line with error bars). As a reference, model NBH01 has been plotted in these panels (solid lines without error bars) to show how the central black hole modifies the structure of the galaxy beyond its central region. Clearly, the black hole tends to destroy any signature of triaxiality in the central region of the collapsed system. However, there are no clear differences between a model with a primordial black hole and one where a black hole grows adiabatically.

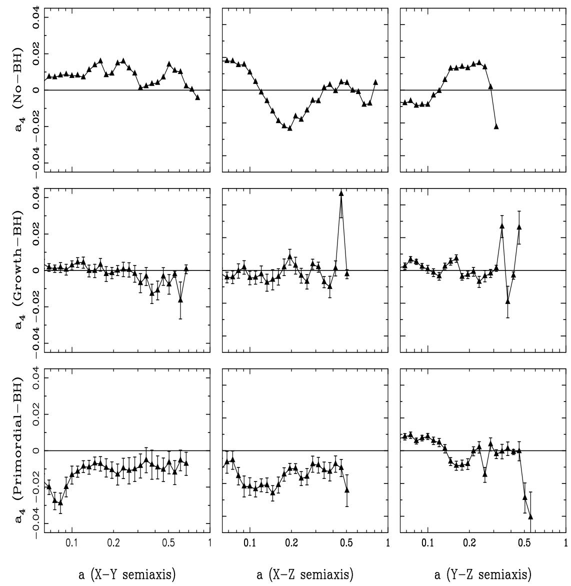

Fig. 2. Parameter a_4 as function of the projected distance along the major semiaxis. Top, middle and bottom panels correspond to our models NBH01, ABH01 and PBH01, respectively.

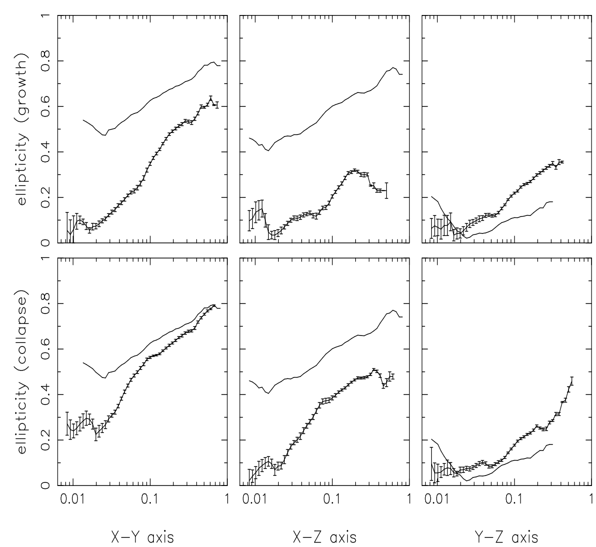

Fig. 3. Ellipticity as function of the projected distance along the major semiaxis. Top and bottom panels correspond to our models ABH01 and PBH01, respectively. Lines without error bars correspond to our control model NBH01.

4. KINEMATICS

The kinematical properties of our models are computed from the projected velocities along the main axes. The line-of-sight velocity distributions

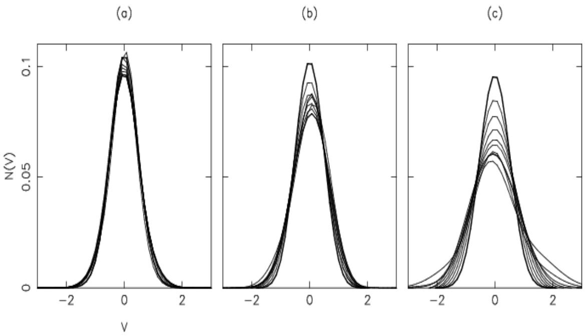

Fig. 4. LOSVDs of our final models taken along the main projected intermediate axis. Panels (a), (b) and (c) correspond to models NBH01, PBH01, and ABH01, respectively. Each panel includes ten lines corresponding to a circular aperture centered on the BH, and on the center of mass of the system for model NBH01.

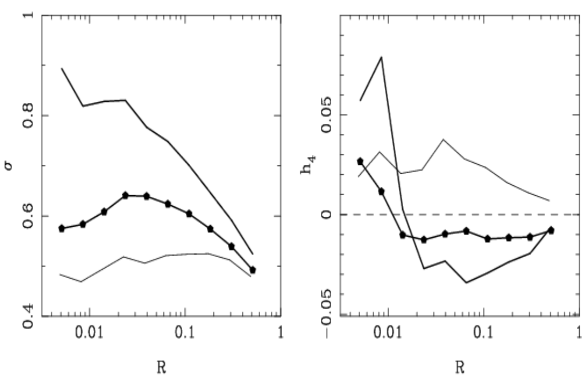

Fig. 5. Velocity dispersion σ (left panel) and the fourth Gauss-Hermite moment h_4 (right panel) as a function of the aperture diameter, D, for models NBH01 (thin line), PBH01 (thick line with dots) and ABH01 (thick line).

(LOSVDs) are recovered using a nonparametric technique of Maximum Penalized Likelihood (MPL) (see Merritt 1997 for a more detailed description of this method). To do this, the MPL estimate, $\hat{N}(V)$, of an LOSVD is determined on a velocity grid by maximizing the log likelihood of the distribution of projected velocities along the line of sight over an aperture and subject to a penalty function that measures the lack of smoothness of $\hat{N}(V)$. Once that $\hat{N}(V)$ is obtained, it is expanded into its Gauss-Hermite moments (GH) as defined by Gerhard (1993) by the prescription given by van der Marel & Franx (1993). In particular, the quantities relevant to our study are the mean velocity, V_0, the velocity dispersion, σ_0, and the odd and even first-order departures from a Gaussian distribution, h_3 and h_4, respectively.

Figure 4 shows the LOSVDs of our final models NBH01, PBH01 and ABH01 (from left to right), respectively, evaluated along the main intermediate projected axis. Each line corresponds to a different circular aperture centered on the black hole. The aperture radii span from $2r_{bh}$ to the projected half-mass radius.

For all apertures, the family of LOSVDs in Figure 4(a) exhibits almost the same Gaussian profile with a sharp peak and an almost nonexistent wing. Panels (b) and (c) show the effect of a central black hole. It can be noticed that the LOSVDs present broader wings and shallower peaks as the aperture decreases. For model ABH01 this effect is more noticeable compared to model PBH01.

Figures 5(a)-(b) correspond to the velocity dispersion σ and to the parameter h_4, recovered from the Gauss-Hermite expansion of the LOSVD, as a function of the aperture radius R. For our model NBH01 (thin line), the velocity dispersion remains almost constant for all apertures with a mean value of ~ 0.5. For models PBH01 (thick line with marks) and ABH01 (thick line) it increases for small apertures. The largest value of the velocity dispersion, $\sigma \approx 0.9$, is found for model ABH01 at an aperture radius of $R \approx 0.002$.

Positive values of h_4 (Figure 5(b)) indicate that the LOSVD is sharp at the center with a slight decay and weak wings; negative values of h_4 show that the LOSVD is broader at the center with steeper edges (see Figure 11.5 Binney & Merrifield 1998). It is observed that model NBH01 has positive values of h_4 for all apertures in agreement with the sharpness of the LOSVDs shown in Figure 4(a). The presence of a central black hole changes this behavior mostly for larger apertures; h_4 is positive for small apertures while for larger ones it is negative, changing its value around an aperture of diameter $\sim 0.01 - 0.015$. These values are quite coincident with the radius of influence of the central black hole of these models, which is about $r_{bh} \sim 0.01$ (in model units) for both models.

Similar trends to the ones reported by van der Marel (1994) for M87 and Milosavljevick & Merritt (2001) for equal-mass mergers are found for both the velocity dispersion and the parameter h_3 as a function of the aperture.

This work is a first approximation to understand how a central super massive black hole could affect the observational characteristics of a triaxial system.

We explore one initial value for the density profile and the M_{bh}/M_b ratio. We expect that the morphology and kinematics will not show important changes at large radii for initial low density profiles. However, is possible that they could be affected at large radii for steep density profiles, where the resulting r_{bh} is large (Cruz & Velázquez 2004) and will show a correlation with radius where h_4 becomes negative (see Fig. 5).

5. SUMMARY

We have carried out a set of numerical simulations to study the effect of a central supermassive black hole on the morphology and kinematics of a triaxial system formed through gravitational cold collapse. We have addressed two models; in one case the central black hole has a primordial origin (*i.e.* it formed before the collapse occurs); in the other case the black hole grows adiabatically once the inner region of the system has relaxed. In general, both systems with a central black hole show values of $a_4 < 0$ (boxy deviations) while the gravitational collapse without a black hole shows values of $a_4 > 0$ (disk deviations) for most of the projections.

On the other hand, the LOSVDs of model NBH01 shows the sharpest peak with negligible wings while the adiabatical growth of the black hole exhibits extended wings with shallower central peaks. This behavior has been quantified with the velocity dispersion and the parameter h_4. It is found that the collapse without a black hole exhibits a nearly constant velocity dispersion for all apertures while the ABH01 shows the most centrally peaked velocity dispersion.

The parameter h_4 is positive for all apertures in the case of the collapse without a black hole, while this parameter changes sign for the gravitational collapse with a central black hole being positive for radii $\leq 0.01 - 0.015$ and negative otherwise. The radius at which h_4 changes its sign seems to be related to the radius of influence of the black hole ($r_{bh} \approx 0.01$).

Finally, in agreement with Stiavelli (1998), it is not possible from these results to differenciate between models with a primordial black hole and those where the black hole grows adiabatically.

We thank the anonymous referee for several suggestion that improved this paper. This research was supported by DGAPA grant IN113403, Universidad Nacional Autónoma de México.

REFERENCES

Aguilar, L. A., & Merritt, D. 1990, ApJ, 354, 33
Bender, R. 1988, A&A, 74, 385
Binney, J., & Merrifield, M. 1998, Galactic Astronomy (Princenton: Princenton Univ. Press)
Cretton, N., et al. 2001, ApJ, 554, 291
Cruz, F., & Velázquez, H. 2004, ApJ, 612, 593
________. 2005, RevMexAA, 41, 25
Dorband, N., Hemsendorf, M., & Merritt, D. 2003, J. Comp. Phys., 185, 484
Faber, S., et al. 1997, AJ, 114, 1771
Ferrarese, L., & Merritt, D. 2000, ApJ, 539, L9
Gebhardt, K., et al. 2000, ApJ, 593, L13
Gerhard, O. E. 1993, MNRAS, 265, 213
Green, P. J., & Silverman, B. W. 1994, Nonparametric Regression and Generalized Linear Models (London: Chapman & Hall)
Jaffe, W., Ford, H. C., Ferrarese, L., van den Bosch, F. C., & O'Connell, R. W. 1994, AJ, 108, 1567
Khochfar, S., & Burkert, A. 2005, MNRAS, 359, 1379
Kormendy, J., & Gebhardt, K. 2001, in AIP Conf. Proc. 586, 20th Texas Symposium on Relativistic Astrophysics, ed. H. Martel & J. C. Wheeler (New York: AIP), 363
Kormendy, J., & Richstone, D. 1995, ARA&A, 33, 581
Lauer, T. R., et al. 2005, AJ, 129, 2138
Magorrian, J., et al. 1998, AJ, 115, 2285
Marconi, A., & Hunt, L. K. 2003, ApJ, 589, 21
McLure, R. J., & Dunlop, J. S. 2002, MNRAS, 331, 795
Merritt, D. 1997, AJ, 114, 228
Merritt, D., & Ferrarese, L. 2001, MNRAS, 320, L30
Merritt, D., & Quinlan, Q. 1998, ApJ, 498, 625
Milosavljevic, M., & Merritt, D. 2001, ApJ, 563, 34
Naab, T., & Burkert, A. 2003, ApJ, 597, 893
Naab, T., Burkert, A., & Hernquist, L. 1999, ApJ, 523, L133
Stiavelli, M. 1998, ApJ, 495, L91
Udry, S. 1993, A&A, 268, 35
van Albada, T. S. 1982, MNRAS, 201, 939
van der Marel, R. P. 1994, ApJ, 432, L91
van der Marel, R. P., & Franx, M. 1993, ApJ, 407, 525
Velázquez, H., & Aguilar, L. A. 2003, RevMexAA, 39, 197

Héctor Aceves, Fidel Cruz, and Héctor Velázquez: Instituto de Astronomía, Universidad Nacional Autónoma de México, Apdo. Postal 877, 22860 Ensenada, B. C., Mexico (aceves, fidel, hmv@astrosen.unam.mx).